The wide-angle point spread function of the human eye reconstructed by a new optical method

Harilaos Ginis Institute of Vision and Optics, University of Crete, Heraklion, Crete, Greece

Guillermo M. Pérez Laboratorio de Optica, Centro de Investigación en Óptica y Nanofísica, Universidad de Murcia, Murcia, Spain

Juan M. Bueno Laboratorio de Optica, Centro de Investigación en Óptica y Nanofísica, Universidad de Murcia, Murcia, Spain

Pablo Artal Laboratorio de Optica, Centro de Investigación en Óptica y Nanofísica, Universidad de Murcia, Murcia, Spain

The point spread function (PSF) of the human eye spans over a wide angular distribution where the central part is associated mostly to optical aberrations while the peripheral zones are associated to light scattering. There is a plethora of optical methods for the direct and indirect measurements of the central part of the PSF as a result of monochromatic and polychromatic aberrations. The impact of the spatial characteristics of this central part of the PSF on the retinal image quality and visual function has been extensively analyzed and documented both by optical and psychophysical methods. However, the more peripheral areas of the PSF in the living human eye, ranging from about 1 to 10 degrees of eccentricity, have been investigated only psychophysically. We report here a new optical method for the accurate reconstruction of the wide-angle PSF in the living human eye up to 8 degrees. The methodology consists of projecting disks of uniform radiance on the retina, recording the images after reflection and double pass through the eye's optics and performing a proper analysis of the images. Examples of application of the technique in real eyes with different amount of scatter artificially induced are presented. This procedure allows the direct, accurate, and in vivo measurement of the effect of intraocular scattering and may be a step toward the comprehensive optical evaluation of the optics of the living human eye.

Keywords: light scattering, optics, human eye, straylight, optical methods

Citation: Ginis, H., Pérez, G. M., Bueno, J. M., & Artal, P. (2012). The wide-angle point spread function of the human eye reconstructed by a new optical method. *Journal of Vision, 12*(3):20, 1–10, http://www.journalofvision.org/content/12/3/20, doi:10.1167/12.3.20.

Introduction

The optical quality of the retinal image (Artal, Guirao, Berrio, & Williams, 2001) is the first physical factor influencing visual performance. The study of the eye in terms of its optical quality is approached by analyzing both the geometrical characteristics of the ocular surfaces and the intrinsic properties of the media with which the light interacts when passing through the eye. Wavefront sensors provide information on the overall optical quality of the eye through the aberrations. The image of a point source projected onto the retina, the ocular point spread function (PSF), is affected by diffraction in the pupil, aberrations, and scatter. The homogeneity of the ocular structures affects the retinal images, although this fact is not usually taken into account when describing the optical quality only in terms of aberrations (Diaz-Douton, Benito et al., 2006). Light scattering is a phenomenon originated from localized (particle-like) irregularities of the refractive index within the ocular media and leads to the spread of the light at larger angles over the retina. This effect is described by statistical terms (e.g., intensity and angular distribution) rather than by a calculation based on the geometrical characteristics of the eye that can describe quite accurately the aberrations (Tabernero, Berrio, & Artal, 2011). Although aberrations and scatter are often treated separately due to their different origin, under particular experimental conditions or depending on the visual task, they contribute in combination to the retinal image deterioration. It was also shown that is also possible that scatter and aberration may interact to produce an improved retinal image (Perez, Manzanera, & Artal, 2009). In particular, light scattering may have a significant impact on retinal image contrast when the eye is observing scenes in which bright light sources are present. An example of such a condition is the visual environment during night driving. In general, scattered light reduces retinal image quality due to a decrease in the contrast of the retinal images.

doi: 10.1167/12.3.20 Received October 6, 2011; published March 26, 2012 ISSN 1534-7362

Since the PSF contains all the relevant information from both aberrations and scatter, it has been a long history trying to directly record it in the living eye (Campbell & Gubisch, 1966; Flamant, 1955) using the ophthalmoscopic or double-pass approach. This technique (Santamaria, Artal et al., 1987) is based on projecting a point source on the retina and recording the reflected image after double pass through the eye with a camera conjugated with the retina. As the PSF is imaged through the optics of the eye, the resulting double-pass image is the autocorrelation of the PSF (Artal, Marcos et al., 1995). Based on this approach, measurement of light scattering in the eye can be performed by analyzing the intensity recorded at the peripheral part of the double-pass PSF in respect to the total intensity (Westheimer & Liang, 1994). This technique has proved useful for the quantification of scattering in situations with a significant presence, such as in cataract patients (Artal, Benito et al., 2011) and in dry eye for the characterization of tear film quality (Benito, Perez et al., 2011). The main limitation in this technique is not conceptual but practical. It arises from the extremely broad dynamic range of the PSF in the human eye that poses inherent difficulties in imaging both the central and peripheral areas of the PSF simultaneously. Practically, even with state-of-the-art detectors, scattered light intensities are above the noise level only for relatively small angles around the peak of the image. Beyond this angle, typically around 1 degree, the light in the PSF in the normal eye is so dim that it is not directly measurable. This limits the analysis of the scattered light from double-pass images to the central few tens of minutes of arc. An additional limitation arises from the fact that as the retinal image is analyzed, diffuse light from deeper layers (such as the choroid) may be interpreted as scattered light in the optics and therefore result to an overestimation of the optical PSF for these angles. This effect is less important when using shorter wavelengths (Lopez-Gil & Artal, 1997) since the diffuse light is strongly attenuated and confined due to the increased absorbance of hemoglobin (Delori & Pflibsen, 1989; Hodgkinson, Greer et al., 1994). Similar limitations are found in light scattering measurements based on the analysis of the images acquired by Hartmann–Shack wavefront sensors (Nam, Thibos et al., 2011; Thibos & Hong, 1999). Then, the measurement of the ocular light scattering based on the double-pass technique using a point source is particularly suitable for those cases in which the amount of scatter is relatively high, such as cataracts or dry eye patients, but is characterized by low signal-to-noise ratio and possible bias (due to retinal diffusion) in eyes with clear media. Alternative optical methods have been proposed based on the analysis of Purkinje images (Bueno, De Brouwere et al., 2007) or the dynamic light scatter measurements (Ansari & Datiles, 1999; Datiles, Ansari et al., 2008), but these methods analyze backscattered light rather than the visually relevant-forward scattered light.

Several psychophysical methods to quantify intraocular scattering causing glare and influencing a visual task have been reported. Among these, the brightness visual acuity test (Holladay, Prager et al., 1987) assesses the effect of light scattering by means of the decrease in visual acuity caused by a controlled glare source. In this method, the subject's visual acuity is assessed while the subject's eye is positioned at the center of light diffusing semi-sphere and observes the optotype through a small hole. Light diffused at the semi-sphere generates a uniform glare veil with adjustable luminance. The impact of different levels of the glare source luminance in visual functions such as visual acuity can be used to infer the severity of intraocular light scatter. In particular, the influence of glare sources on low-contrast visual acuity has been studied (Bailey & Bullimore, 1991). The most standardized and documented psychophysical procedures specifically designed for the quantification of intraocular light scattering are the direct compensation method (van den Berg, 1986) and the compensation comparison method (Franssen, Coppens et al., 2006). Both methods are based on the principle of equivalent luminance caused by a flickering glare source that the subject matches to the adjustable luminance of a test object that is flickering in counter-phase. In the direct compensation method, a flickering annular glare source subtending an angle of about 7 deg is creating a flickering veiling glare. A circular test field positioned at the center of the annulus has adjustable luminance flickering in counter-phase to the glare annulus. The subject is requested to adjust the luminance of the test object in order to null the flickering. The luminance required to null the flickering is equal to the veiling glare produced by light scattering at 7 deg. In the compensation comparison method, the central test field is divided in two semi-disks and different amount of compensating light is presented to each half. The psychophysical procedure involves a series of forced-choice responses where the subject selects the semi-disk with the stronger flicker. The equivalent luminance is estimated by means of fitting an appropriate psychometric function to the subjects' responses. The compensation comparison method has been used in numerous studies (Guber, Bachmann et al., 2011; van den Berg, Franssen et al., 2009). One limitation related to the psychophysical nature of the tasks is the possible complexity for some subjects.

In the present work, we have developed a new optical methodology for the reconstruction of the wide-angle PSF in the living human eye. The present method overcomes the limitations of the existing optical techniques by incorporating extended light sources that are imaged onto the retina and image analysis to reconstruct the PSF at eccentric angles. In this manner, more light can be used to illuminate the retina and the effect of light scattering can be calculated without having to deal with the extremely high dynamic range of the PSF. We demonstrate that this

new instrument and measurement procedure is able to measure the intensity of the intraocular scattered light at large angles. This is a step toward the comprehensive evaluation of the optics of the human eye and its impact in vision.

Methods

Theoretical background

The basic concept implemented here is the projection of extended sources (uniform disks) onto the retina and imaging these disks in a double-pass configuration. The recorded image is the convolution of the projected disk with the autocorrelation of the PSF of the eye under investigation. Assuming the disk (before convolution) has a uniform intensity equal to I_o and subtends on the retina a visual angle equal to ϑ (radius), the intensity at the center of the disk as recorded at the camera plane is given by the following equation:

$$I_c(\vartheta) = I_o \int_0^{\vartheta} 2\pi\varphi \mathrm{PSF}_{dp}(\varphi) d\varphi, \quad (1)$$

where $I_c(\vartheta)$ is the intensity at the center of the disk (which depends on the radius of the projected disk) and $\mathrm{PSF}_{dp}(\phi)$ is the double-pass PSF of the eye. With reference to Figure 1, this value is also equal to the surface integral of the PSF within a circle of radius ϑ. Assuming that the integral of the PSF (either single pass or double pass) for

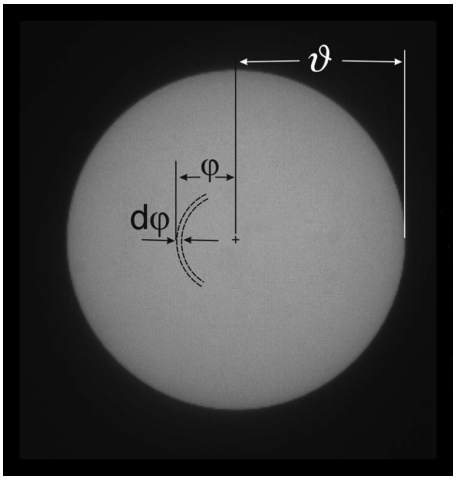

Figure 1. A uniform disk imaged through a system with a rotationally symmetric PSF that includes scatter. The intensity at the center of the disk is given by Equation 2. I_c is also equal to the fraction of energy of the PSF encircled by a circle having the radius of the disk.

$\vartheta = \pi/2$ is equal to unity, it can be shown that the central intensity of an infinite disk is equal to I_o. Qualitatively, this means that while for a small patch the central intensity is attenuated by light scattering this intensity is increased as peripheral annuli are added to the patch and scattered light from the annuli is complemented to the center of the patch.

In an experimental situation where the analysis spans several degrees (i.e., about 10 degrees), it is a reasonable approximation to assume that effectively all the energy of the PSF is taken into account and therefore all measurements of I_c can be normalized in respect to the largest available disk. This assumption is supported by existing models of the PSF in the human eye (van den Berg, Hwan et al., 1993; Vos & van den Berg, 1999).

Therefore, Equation 1 becomes simply

$$I_c(\vartheta) = \int_0^{\vartheta} 2\pi\varphi \mathrm{PSF}_{dp}(\varphi) d\varphi, \quad (2)$$

where $I_c(\vartheta)$ denotes the normalized intensity in respect to the central intensity of the largest disk. Of course, I_c in this case takes values between 0 and 1.

In the proposed approach, a series of disks with increasing ϑ ranging from 0.18 to 8.1 degrees is projected onto the retina. If I_c is known experimentally, then the PSF can be retrieved from Equation 2 by taking its derivative in respect to ϑ:

$$\mathrm{PSF}_{dp}(\vartheta) = \frac{1}{2\pi\vartheta} \frac{dI_c(\vartheta)}{d\vartheta}. \quad (3)$$

Finally, the PSF of the system can be retrieved from the double-pass PSF by considering this as the autocorrelation of the PSF and assuming rotational symmetry:

$$\mathrm{PSF} = \mathbb{F}^{-1}\left[\sqrt{|\mathbb{F}(\mathrm{PSF}_{dp})|}\right], \quad (4)$$

where $\mathbb{F}$ and $\mathbb{F}^{-1}$ denote 2-dimensional Fourier and inverse Fourier transforms, respectively.

Data processing

Two different methodologies can be followed for treating experimental data of I_c (or the radial integral of the PSF). A straightforward method is to approximate the derivative in Equation 3 with finite differences:

$$\mathrm{PSF}_{dp}(\vartheta_n) = \frac{1}{2\pi\vartheta_n} \frac{I_c(\vartheta_{i+1}) - I_c(\vartheta_i)}{\vartheta_{i+1} - \vartheta_i}, \quad (5)$$

where ϑ_i are the radii of the consecutive disks, and $\vartheta_n = (\vartheta_{i+1} + \vartheta_i)/2$.

Alternatively, an appropriate function can be fitted to the data of I_c and the derivative can then be evaluated analytically. An appropriate function for I_c can be found by using one of the known models (IJspeert, van den Berg, & Spekreijse, 1993) for glare and by using Equation 2.

Given that our data represent a small angular range, we have used a simplified power law function to approximate the PSF:

$$\mathrm{PSF}(\vartheta) = (1 - a)\mathrm{PSF}_{\mathrm{dl}} + a\left(\frac{b}{(\vartheta + \vartheta_0)^n}\right), \quad (6)$$

where $\mathrm{PSF}_{\mathrm{dl}}$ is the diffraction-limited PSF (calculated based on the apertures of the system and radially normalized to 1), a is a coefficient of scatter, ϑ_o is an arbitrary small angle (to avoid the singularity at $\vartheta = 0$), n is approximately 2, and b is a normalization coefficient so that the scattering law is radially normalized ($\int_0^{\tau/2} 2\pi\vartheta\left(\frac{b}{(\vartheta+\vartheta_o)^n}\right)d\vartheta = 1$). We assume that a function of this form can be applied for the numerical approximation of both the single- and double-pass PSF of the eye in relation to scatter. The small angle part of this formula is dominated by an Airy pattern (consistent with the use of small diaphragms in our experimental setup). The wide-angle part of this formula is a generalization of the age-adapted Stiles–Holaday formula (Vos & van den Berg, 1999). With appropriate adjustments of the parameters a, n, and ϑ_o, this formula produces—practically—identical numerical values with other functions in the literature for the range of angles assessed with our method (0–9 degrees).

For practical applications, the value of the double-pass PSF at a given angle (e.g., 5 degrees) can be used as a measure of the intensity of the scattered light in the eye. This value can be calculated as in Equation 5 by approximating the derivative with the slope of a linear function fitted to a region of angles:

$$\mathrm{PSF}_{\mathrm{dp}}(\vartheta_o) = \frac{\mathrm{slope}|_{\vartheta_o}}{2\pi\vartheta_o}. \quad (7)$$

Since this method is considered to be less sensitive to noise, it was used for the analysis of the below results.

Experimental setup and procedure

Figure 2 shows the experimental setup used to project the disks on the retina and record the double-pass images. Each disk is generated by a liquid crystal modulator (LCOS 2002, Holoeye, Germany) that is back-illuminated by a Xenon lamp. Appropriate optical filters were used to select a band of green light (530 ± 30 nm FWHM). The light distribution is made uniform at the plane of the LCOS by means of collimating optics (C) and diffusers (D). The disk uniformity was confirmed to be within 5% of the mean by introducing a camera at the retinal plane during the preparation of the experimental setup. On the first pass, the light passes lenses L1, L2, and L3 and enters the eye and the image of the extended object is formed on the retina. Diaphragm D1 is conjugated with the pupil plane of the eye (by lenses L2 and L3) and therefore controlling the part of the pupil that is used for the object

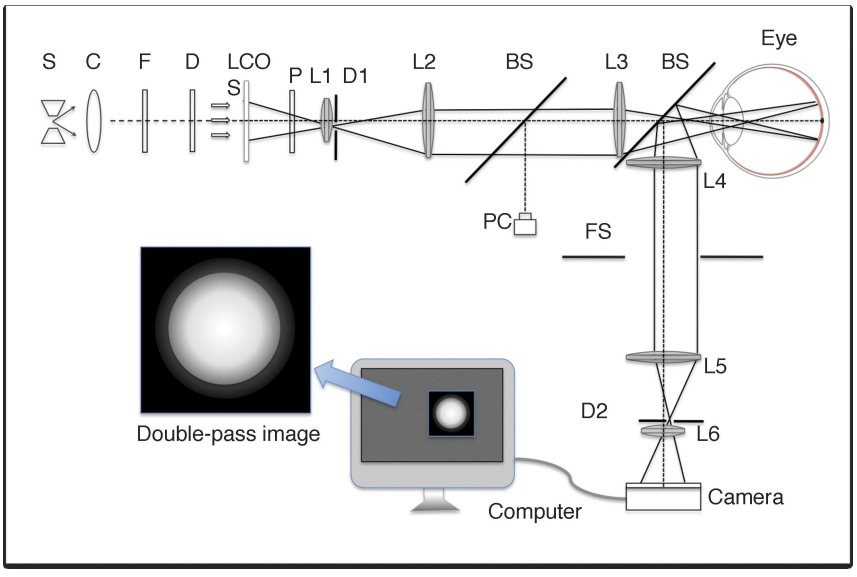

Figure 2. Experimental setup. S, light source; C, collimating lens; F, green filters; D, diffuser; LCOS, liquid crystal spatial light modulator; P, linear polarizer; L1–L6, lenses; D1 and D2, diaphragms; BS, beam splitters; PC, pupil camera; FS, field stop.

projection. In the second pass, the image of the disk at the retina is imaged onto an electron multiplying CCD camera (EMCCD Luca, Andor, UK) through beam splitter BS and lenses L4, L5, and L6. Diaphragm D2 is conjugated with the pupil plane by lenses L4 and L5 and controls the part of the pupil used for imaging the retina. D1 and D2 are displaced transversely to each other so that a different part of the pupil is used for projection (first pass) and recording (second pass). The two sub-apertures have diameters equal to 2 mm and their centers are separated by 4 mm (i.e., a minimum of 6-mm pupil is required for image acquisition for this particular experimental configuration). When the two sub-apertures are spatially separated at the pupil plane, backscattering from the cornea and the lens is removed from the recorded retinal images. Without this strategy, light from the anterior segment reflections would degrade all the recorded images, invaliding the whole procedure.

The dimensions of the disks on the spatial light modulator were computer controlled and synchronized with image acquisition. In each recorded double-pass image, the intensity at the center of each disk was computed by averaging the central 3 × 3 pixels. The camera's response to light at the particular exposure time and gain of the intensifier was measured in a separate experiment and taken into account by applying a non-linear intensity transformation to the images. The intensity at the center of each disk was normalized in respect to the intensity of the largest available disk, creating then an experimental data set for $I_c(\vartheta)$ (as in Equation 2). The derivative of this intensity with respect to the disk radius was numerically estimated by fitting a linear function to two regions of angles (0.5–2 and 2.5–8 degrees) and applying Equation 7. The particular values of the computed double-pass PSF at 1.25 and 5.25 degrees are reported as parameters to quantify the amount of intraocular scatter.

After proper calibrations and testing of the whole procedure in the artificial eyes, the method was applied in normal subjects. The experiment followed the tenets of the Declaration of Helsinki. Informed consent was obtained by the subjects after they were fully informed about the nature and the possible consequence of the measurements. Two drops of 1% tropicamide were instilled to each tested eye for pupil dilation. The eye pupil was aligned by means of a pupil camera (PC in Figure 2). The subjects fixated on a target that was deliberately displaced to avoid retinal blood vessels at (or near) the center of the projected disks. For each measurement, a sequence of fifty disks corresponding to visual angles ranging from 0.18 to 8.1 deg was recorded. For each image, the exposure time was 300 ms and the subject was allowed to blink between images. The irradiance at the corneal plane was below 20 μW/cm^2. A bite bar mounted on a three-axis positioning stage was used to stabilize the subject's head during measurements.

For the validation of the method and the experimental setup, we measured a reference scattering filter introduced in an artificial eye that had no nominal scattering. Nine measurements were performed with and without the filter. The scattering filter used with the artificial eye was a Black Pro Mist 2 (The Tiffen Company, Hauppauge, NY, USA). This filter has been documented (de Wit, Franssen et al., 2006) to have scattering properties (angular distribution and magnitude) similar to a young healthy eye (straylight parameter equal to 0.88). Three eyes of three subjects (GP, JB, and CS) were measured. Two of the subjects were measured repetitively (GP: nine times, JB: five times) to demonstrate the repeatability of the method in human eyes. For one subject (GP), the consecutive measurements were repeated while the subject was wearing two different light-scattering contact lenses (CLs).

These are custom-made rigid gas-permeable CLs (Menicon, Japan) with different concentrations of glass microspheres with diameters ranging from 1 to 20 μm in their RGP material. The CLs have no refractive power. Their scattering properties have been measured in a separate experiment both optically (Bueno et al., 2007) and psychophysically (by means of the commercially available instrument C-Quant) and were found to contribute with amounts of scatter consistent with normal or

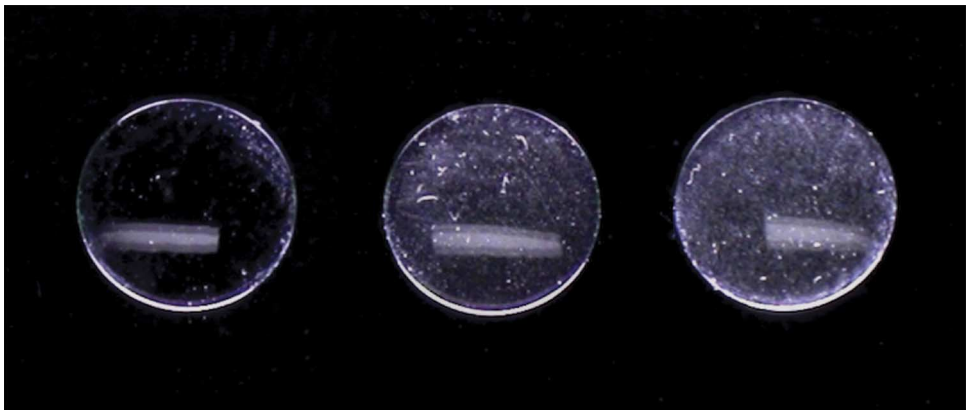

Figure 3. Dark-field photograph of the rigid gas-permeable contact lenses that were used to introduce additional light scattering.

mildly scattering eyes (0 to 0.6 log units increase of the straylight parameter as in Franssen et al., 2006). Figure 3 shows a dark field photograph of the CLs used here, where differences in the scattering produced can be observed.

Results

Figure 4 shows the experimental data and the corresponding fittings for two normal young subjects. It can be observed how the procedure here reported is able to discriminate different amounts of scattering for both eyes despite being normal young subjects. As an example, a video of the retinal images of the projected disks for one of the subjects (GP) is also included (Movie 1).

Figure 5a depicts two sets of experimental data for the same subject corresponding to a naked eye and wearing a CL providing moderate level of scattering. Solid lines are the fittings by the integral of a function as defined in Equation 6. Figure 5b summarizes the results on the estimated value of the double-pass PSF at 5.25 degrees (Equation 7) for the artificial eye as well as for the subjects that were measured repetitively. This value can be used to quantify the intensity of scattered light. The results for smaller angles (e.g., 1.25 degrees) exhibit similar variability and relative magnitude. The double-pass PSF for the artificial eye was found to be essentially zero. This small value represents the ghost reflections and the scattered light in the experimental setup as well as diffuse light in the room. The Black Pro Mist 1 filter introduced to the system light scattering smaller but comparable to that of the normal young eyes (GP and JB) as expected. The additional scattering associated to the scattering contact lenses although very small (equivalent

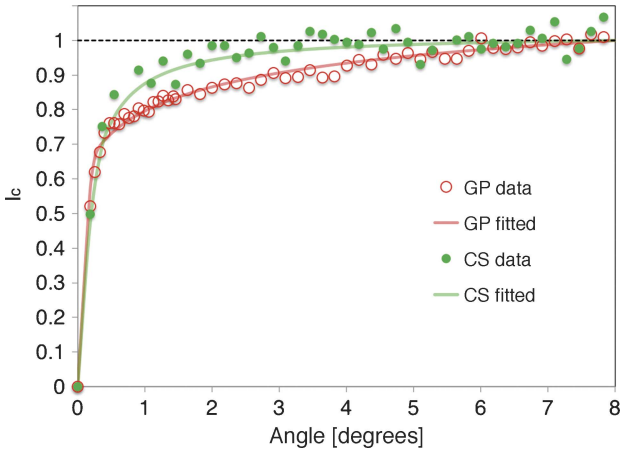

Figure 4. Experimental data acquired for two different subjects and associated fitted functions.

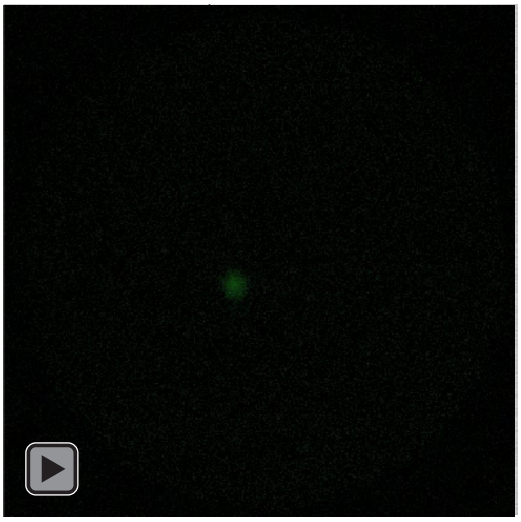

Movie 1. Sequence of disks projected on the retina and recorded in double pass. The diameter (and exact position of the field stop) does not interfere with the analysis of the center of the disk.

to 0.3 and 0.6 log units of the psychophysical straylight parameter) could be systematically measured. The variability of the measurements is shown in Figure 5b where the first and third quartiles of the measurements correspond to the height of each box.

It should be noted that all the information obtained from the experimental data correspond to the light passing twice the ocular media. This fact might lead to an increase in the measured scattering and then to an overestimation of the actual values of the scatter parameters. However (as shown above) with our procedure, not only the PSF in double pass can be directly computed, but also the actual

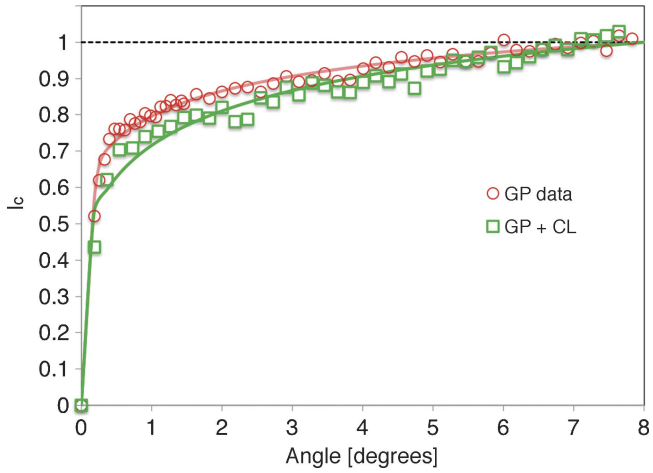

Figure 5a. Experimental data on the radial integral of the PSF for one eye under two experimental conditions: no CL (red symbols) and wearing a CL with moderate scattering. Red symbols are the same as in Figure 4.

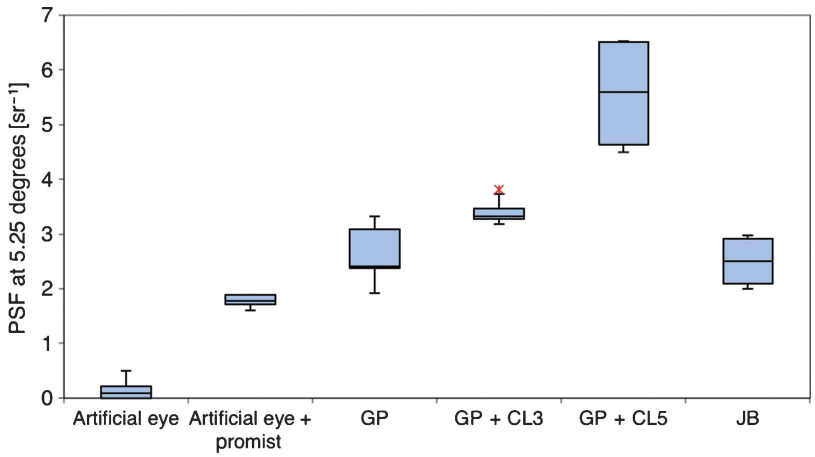

Figure 5b. Double-pass PSF calculated at 5.25 degrees for the artificial eye and the human eyes under different additional scattering conditions.

PSF in single pass can also be estimated. The latter will inform on the actual contribution of the scattering, avoiding the influence of the second pass.

In this sense, the analytical derivative of the function of the fitting of the experimental data (solid lines in Figures 4 and 5) is used to calculate the two-dimensional rotationally symmetric double-pass PSF (Equation 3). Finally, Equation 4 is used to calculate the corresponding single-pass (reconstructed) PSF. For one of the subjects involved in this study, Figure 6 presents the PSFs in double and single passes.

Finally, Figure 7 shows the reconstructed PSF for the two subjects in Figure 5 together with those corresponding to two existing models in the literature.

Discussion

An all-optical experimental procedure for the measurement of the PSF of the human eye in an angular range up to 8 degrees has been developed. This allows the reconstruction of a part of the PSF spanning about six orders of magnitude in intensity. The PSF at angles larger than about 1 degree is unlikely to be influenced by aberrations and artifacts related to light diffusion in the choroid. As far as we know, these are the first wide-angle PSF reconstructed from optical data in the eye.

Results here shown demonstrate the sensitivity of the reported procedure especially when wider ranges of angles are taken into account. It is interesting to notice that the linear fit across a range of angles suggests that the PSF is constant across this range. This may lead to an overestimation of the actual value of the PSF at the reported angle, as the PSF varies with angle as a power law. Moreover, the values reported in Figure 5b refer to the double-pass PSF and should not be interpreted directly as the PSF of the eye at these angles.

In the experimental setup, particular attention was paid to the spatial separation of the illuminating and imaging light pathways in order to avoid backscattering that might contaminate the measurements and lead to erroneous interpretations. The incoming–outgoing spatial separation was possible for the cornea and the crystalline lens; however, a partial overlap still occurs at the vitreous. Although it is possible that in eyes with severe floaters, light scattering from the vitreous is significant (Mura, Engelbrecht et al., 2011), it is reasonable to hypothesize that in healthy eyes it is negligible compared to the forward scattering from the cornea and the lens (DeMott & Boynton, 1958; Ritschel, Ihrke et al., 2009). To achieve this spatial separation, two circular sub-apertures

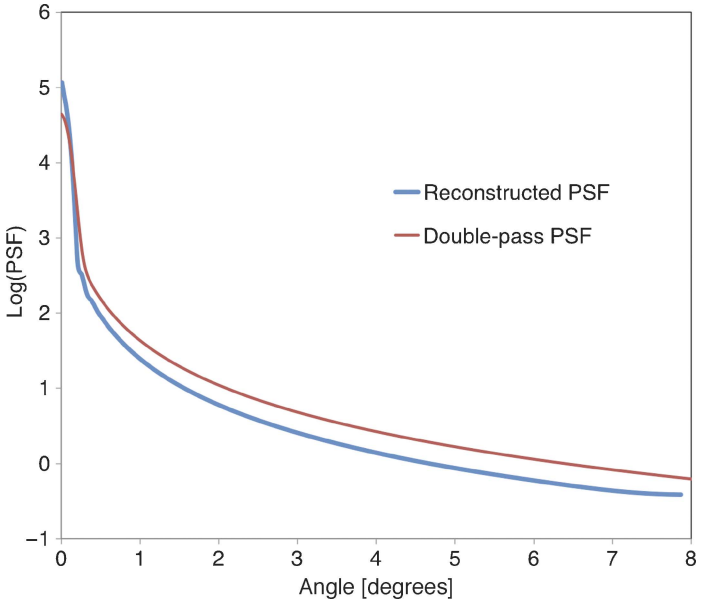

Figure 6. Double- and single-pass PSFs for subject GP (raw data in Figure 5—no CL).

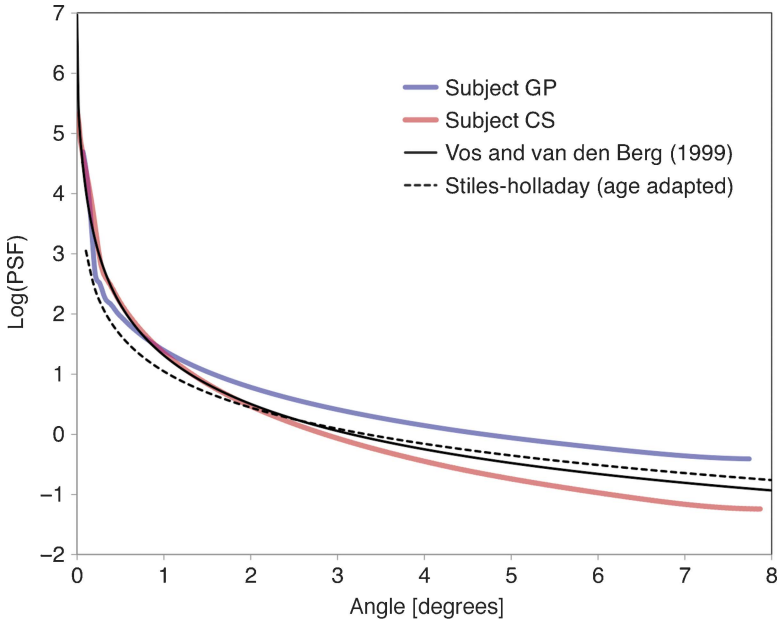

Figure 7. Comparison between two reconstructed PSFs (red and blue lines) based on data here recorded and those corresponding to two existing models in the literature (solid and dashed black lines). (Equations from Vos & van den Berg, 1999.)

conjugated to the pupil plane and laterally displaced to each other in the vertical orientation (Figure 2) were employed. The small diameter of these sub-apertures (2 mm) allowed us to assume that the effect of aberrations was minimal and that the central part of the PSF corresponded to a diffraction-limited system for both the illumination and the imaging arm. This assumption helped simplify the PSF model (Equation 6). The fact that only a fraction of the pupil is used does not seem to pose limitations to the procedure, as in terms of scatter, the PSF does generally not depend on pupil diameter (Franssen, Tabernero et al., 2007). However, in the case of non-uniform distribution of scatterers such as in corneal scars or localized cataract opacities, this approach may lead to an overestimation or underestimation of scattering depending on whether these defects are on the measurement paths or not. The wide-angle PSF derived by our method is calculated based on light transmitted through the optics of the eye. This might give rise to differences from the glare functions derived psychophysically as typically the later incorporate additional light that is transmitted through the iris and the sclera reaching the fovea and contributing to the veiling glare.

Light diffusion in the retina and the choroid can affect all measurements where the retina ideally would behave like as a partially reflective uniform surface. Especially in cases where the spatial distribution of light is evaluated, this may lead to an increase in the size of the estimated PSF. An additional source of error may arise from the irregularity of the reflectance of the fundus that may be affected by the distribution of macular pigment, irregular pigmentation patches, or by the presence of large vessels near the area analyzed. In our approach, the green wavelength minimized the effect of diffusion in the choroid. Large vessels near the analyzed patch were avoided by appropriate positioning of the fixation target.

It is feasible to envisage the adaptation of this new methodology in an instrument suitable for clinical application. The procedure can be fast and does not require the active participation of the subject as it is the case for psychophysical procedures. This fact is of particular importance, especially as clinical assessment of the intraocular scattering is mostly practiced in elderly patients.

The optical instrument and methodology here implemented can be useful for a further understanding of phenomena associated to light scattering and glare. In particular, it may be used for the analysis of wavelength dependence of intraocular scattering, to study the effect of diffusion at the choroid in the optical PSF of the human eye, and most importantly, to explore differences between the optical and psychophysical PSFs of the human eye in large angles and the role of the Stiles–Crawford effect in suppressing diffuse light both from the optics and in the fundus.

Conclusions

A new, accurate, and objective optical method to reconstruct for the first time the wide-angle PSF in the human eye has been developed and demonstrated. The approach can be used to measure scatter in the eye. The procedure is sensitive enough to detect differences in the light scatter intensity between normal healthy eyes in vivo and may be a step toward the comprehensive optical evaluation of the optics of the human eye.

Acknowledgments

This work has been supported by "Ministerio de Educación y Ciencia," Spain (Grants FIS2010-14926 and CSD2007-00013) and "Fundación Séneca," Murcia, Spain (Grant 04524/GERM/06). One of the authors (HG) acknowledges the fellowship from "Fundación Séneca" (Grant 14835/IV10/10) to visit the University of Murcia.

Commercial relationships: none.
Corresponding author: Harilaos Ginis.
Email: ginis@ivo.gr.
Address: Institute of Vision and Optics, University of Crete, Voutes Campus, Heraklion 71003, Greece.

References

Ansari, R. R., & Datiles, M. B., III (1999). Use of dynamic light scattering and Scheimpflug imaging for the early detection of cataracts. *Diabetes Technology & Therapeutics, 1,* 159–168.

Artal, P., Benito, A., Perez, G. M., Alcon, E., De Casas, A., Pujol, J., & Marin, J. M. (2011). An objective scatter index based on double-pass retinal images of a point source to classify cataracts. *PLoS ONE, 6,* e16823.

Artal, P., Guirao, A., Berrio, E., & Williams, D. R. (2001). Compensation of corneal aberrations by the internal optics in the human eye. *Journal of Vision, 1*(1):1, 1–8, http://www.journalofvision.org/content/1/1/1, doi:10.1167/1.1.1. [PubMed] [Article]

Artal, P., Marcos, S., Navarro, R., & Williams, D. R. (1995). Odd aberrations and double-pass measurements of retinal image quality. *Journal of the Optical Society of America A, Optics, Image Science, and Vision, 12,* 195–201.

Bailey, I. L., & Bullimore, M. A. (1991). A new test for the evaluation of disability glare. *Optometry Visual Science, 68,* 911–917.

Benito, A., Perez, G. M., Mirabet, S., Vilaseca, M., Pujol, J., Marin, J. M., & Artal, P. (2011). Objective optical assessment of tear-film quality dynamics in normal and mildly symptomatic dry eyes. *Journal of Cataract & Refractive Surgery, 37,* 1481–1487.

Bueno, J. M., De Brouwere, D., Ginis, H., Sgouros, I., & Artal, P. (2007). Purkinje imaging system to measure anterior segment scattering in the human eye. *Optics Letters, 32,* 3447–3449.

Campbell, F. W., & Gubisch, R. W. (1966). Optical quality of the human eye. *The Journal of Physiology, 186,* 558–578.

Datiles, M. B., 3rd, Ansari, R. R., Suh, K. I., Vitale, S., Reed, G. F., Zigler, J. S., Jr., & Ferris, F. L., 3rd (2008). Clinical detection of precataractous lens protein changes using dynamic light scattering. *Archives of Ophthalmology, 126,* 1687–1693.

Delori, F. C., & Pflibsen, K. P. (1989). Spectral reflectance of the human ocular fundus. *Applied Optics, 28,* 1061–1077.

DeMott, D. W., & Boynton, R. M. (1958). Sources of entoptic stray light. *Journal of the Optical Society of America A, 48,* 120–125.

de Wit, G. C., Franssen, L., Coppens, J. E., & van den Berg, T. J. (2006). Simulating the straylight effects of cataracts. *Journal of Cataract & Refractive Surgery, 32,* 294–300.

Diaz-Douton, F., Benito, A., Pujol, J., Arjona, M., Guell, J. L., & Artal, P. (2006). Comparison of the retinal image quality with a Hartmann–Shack wavefront sensor and a double-pass instrument. *Investigative Ophthalmology and Visual Science, 47,* 1710–1716.

Flamant, M. (1955). Étude de la répartition de lumière dans l'image rétinienne d'une fente. *Revue d'Optique, 34,* 433–459.

Franssen, L., Coppens, J. E., & van den Berg, T. J. (2006). Compensation comparison method for assessment of retinal straylight. *Investigative Ophthalmology and Visual Science, 47,* 768–776.

Franssen, L., Tabernero, J., Coppens, J. E., & van den Berg, T. J. (2007). Pupil size and retinal straylight in the normal eye. *Investigative Ophthalmology and Visual Science, 48,* 2375–2382.

Guber, I., Bachmann, L. M., Guber, J., Bochmann, F., Lange, A. P., & Thiel, M. A. (2011). Reproducibility of straylight measurement by C-Quant for assessment of retinal straylight using the compensation comparison method. *Graefe's Archive for Clinical and Experimental Ophthalmology, 249,* 1367–1371. [PubMed]

Hodgkinson, I. J., Greer, P. B., & Molteno, A. C. (1994). Point-spread function for light scattered in the human ocular fundus. *Journal of the Optical Society of America A, Optics, Image Science, and Vision, 11,* 479–486.

Holladay, J. T., Prager, T. C., Trujillo, J., & Ruiz, R. S. (1987). Brightness acuity test and outdoor visual acuity in cataract patients. *Journal of Cataract & Refractive Surgery, 13,* 67–69.

IJspeert, J. K., van den Berg, T. J., & Spekreijse, H. (1993). An improved mathematical description of the foveal visual point spread function with parameters for age, pupil size and pigmentation. *Vision Research, 33,* 15–20. [PubMed]

Lopez-Gil, N., & Artal, P. (1997). Comparison of double-pass estimates of the retinal-image quality obtained with green and near-infrared light. *Journal of the Optical Society America A, Optics, Image Science, and Vision, 14,* 961–971.

Mura, M., Engelbrecht, L. A., de Smet, M. D., Papadaki, T. G., van den Berg, T. J., & Tan, H. S. (2011). Surgery for floaters. *Ophthalmology, 118,* 1894–1894.

Nam, J., Thibos, L. N., Bradley, A., Himebaugh, N., & Liu, H. (2011). Forward light scatter analysis of the eye in a spatially-resolved double-pass optical system. *Optical Express, 19,* 7417–7438.

Perez, G. M., Manzanera, S., & Artal, P. (2009). Impact of scattering and spherical aberration in contrast sensitivity. *Journal of Vision, 9*(3):19, 1–10, http://www.journalofvision.org/content/9/3/19, doi:10.1167/9.3.19. [PubMed] [Article]

Ritschel, T., Ihrke, M., Frisvad, J. R., Coppens, J. E., Myszkowski, K., & Seidel, H.-P. (2009). Temporal glare: Real-time dynamic simulation of the scattering in the human eye. *Computer Graphics Forum, 28,* 183–192.

Santamaria, J., Artal, P., & Bescos, J. (1987). Determination of the point-spread function of human eyes using a hybrid optical–digital method. *Journal of the Optical Society of America A, 4,* 1109–1114.

Tabernero, J., Berrio, E., & Artal, P. (2011). Modeling the mechanism of compensation of aberrations in the human eye for accommodation and aging. *Journal of the Optical Society of America A, 28,* 1889–1895.

Thibos, L. N., & Hong, X. (1999). Clinical applications of the Shack–Hartmann aberrometer. *Optometry & Visual Science, 76,* 817–825.

van den Berg, T. J. (1986). Importance of pathological intraocular light scatter for visual disability. *Documenta Ophthahnologica, 61,* 327–333.

van den Berg, T. J., Franssen, L., & Coppens, J. E. (2009). Straylight in the human eye: Testing objectivity and optical character of the psychophysical measurement. *Ophthalmic and Physiological Optics, 29,* 345–350.

van den Berg, T. J., Hwan, B. S., & Delleman, J. W. (1993). The intraocular straylight function in some hereditary corneal dystrophies. *Documenta Ophthalmologica, 85,* 13–19.

Vos, J. J., & van den Berg, T. J. (1999). *CIE Collection 1999: Vision and colour, physical measurement of light and radiation*. CIE, ISBN 978 3 900734 97 8.

Westheimer, G., & Liang, J. (1994). Evaluating diffusion of light in the eye by objective means. *Investigative Ophthalmology and Visual Science, 35,* 2652–2657.